Exploring the benefits of integrated energy-water management in reducing economic and environmental tradeoffs

Julianne D Quinn[1], Samarth Singh[2], Julianne Quinn[2], Jordan Kern[2], Rosa Cuppari[2], and Greg Characklis[2]

[1]Affiliation not available
[2]University of Virginia

August 01, 2024

Exploring the benefits of integrated energy-water management in reducing economic and environmental tradeoffs

Samarth Singh, Julianne Quinn*, Jordan Kern, Rosa Cuppari and Greg Characklis

University of Virginia, Charlottesville, VA

E-mail: jdq6nn@virginia.edu

July 31, 2024

Abstract. Integrated water-energy management is crucial for balancing socioeconomic and environmental objectives in multi-reservoir systems. Multipurpose reservoirs support clean energy production, recreation, navigation, and flood protection but also disrupt natural water flows and fish migration. As hydropower's role evolves with grid decarbonization, managing these tradeoffs becomes increasingly complex. An integrated model combining economic and environmental factors is essential to inform how to adapt hydropower operations effectively to complement decarbonization of the electric grid. However, existing literature lacks such comprehensive models.

This study introduces an integrated water-energy optimization model using the Columbia River Basin (CRB) and Mid-Columbia (Mid-C) energy market as a case study. The model couples a simulation of operations of 48 CRB reservoirs with a unit commitment/economic dispatch model of the California and West Coast Power system (CAPOW). We employ Direct Policy Search (DPS) and a multi-objective evolutionary algorithm (MOEA) to optimize four objectives: maximize economic benefits from energy production, minimize fossil fuel electricity generation, minimize environmental flow violations, and minimize peak flood levels. Our findings reveal that the integrated model discovers superior operational strategies compared to existing rules, with some policies outperforming current operations on all objectives simultaneously. Insights from the optimized policies include strategies for improved coordination of reservoir operations using storage and inflow data, and the strategic timing of water releases to ensure increased hydropower production leads to less fossil fuel dependence and greater revenue. These results highlight the potential of integrated models to enhance the sustainability of hydropower operations amid a transitioning energy landscape.

1. Introduction

The management of multi-reservoir networks is a critical aspect of water resource management (WRM), with reservoirs serving a wide range of functions, from providing water for irrigation and clean energy to offering flood protection and supporting recreational activities [1, 2, 3]. However, designing operations for reservoirs is

a challenging multi-objective control problem, as the need to balance competing socioeconomic and environmental interests can lead to conflicts [4, 5]. Classic tradeoffs include those between hydropower and flood protection, or economic and environmental objectives [6, 7, 8, 9]. However, different environmental objectives can also conflict with one another. For example, releasing water to maximize hydropower production and reduce fossil fuels emissions may hinder the system's ability to meet subsequent environmental flow requirements, thereby threatening the sustainability of fisheries that depend on natural flows [10, 11, 12].

Improving reservoir operations to balance these objectives has been a primary research focus in WRM for the past several decades (see reviews by Giuliani et al. [13], Castelletti et al. [14], Labadie [15]). Recent advances in model-free, closed-loop optimal control methods like Direct Policy Search (DPS) have made it computationally tractable to optimize operations at multiple reservoirs for conflicting objectives while implicitly capturing uncertainty in stochastic weather forcing [16, 17]. As a result, there have been extensive studies on operating large reservoirs with the goal of supporting multiple needs such as renewable energy, flood control, and irrigation [18, 19, 20, 21, 22]. These studies span the globe's major river basins and have led to policies that do a better job of balancing these often competing priorities.

However, the multiple objectives considered in these studies have focused exclusively on the water system impacts of changing reservoir operations, only considering energy impacts with respect to hydropower generation. They have not captured the interaction of hydropower operations with energy markets, which has proximate consequences for the calculation of both financial impacts of alternative operations on energy distributors, and environmental impacts via fossil fuel emissions. For example, many previous studies in the water systems literature have designed reservoir operations to maximize hydropower production under the assumption that this will correspond to increased revenue [23, 24, 25, 26]. However, this ignores the influence of hydropower availability on the energy mix, electricity markets and electricity prices. In electricity markets dominated by hydropower, energy suppliers and their customers stand to benefit from understanding how changes in reservoir operations impact electricity prices and utility revenue. With respect to fossil fuel generation, hydropower plays a crucial role in a sustainable energy mix by optimizing the use of water resources to reduce reliance on fossil fuels. However, simply maximizing hydropower generation as many studies do [27, 28] won't necessarily minimize fossil fuel generation; reservoirs need to be operated strategically to enhance grid stability and enable the integration of variable renewables like wind and solar to minimize fossil fuel-fired power generation and their associated emissions. Yet previous water systems models haven't quantified the reduction in fossil fuel generation that can be achieved through optimized hydropower operations [29, 30, 31, 32].

In contrast, the energy systems literature addresses how hydropower operations influence energy markets and fossil fuel emissions, but often omits consideration of water system objectives. For example, work in the Brazilian hydroelectric system has

jointly optimized hydropower and thermal generation utilizing stochastic optimization to maximize net spot revenues or expected benefits of reducing thermal generation, but neglects other priorities, such as flood control and environmental flows [33, 34, 35]. An integrated model of the water and energy system is needed that can jointly capture all these conflicting water and energy system objectives and design hydropower operations to balance them.

This study addresses these gaps in existing research by tightly coupling a reservoir operations model with a power systems model and then jointly optimizing operations for multiple objectives using the integrated model. The tight coupling of the integrated model is critical. In a hydropower system, loosely coupling a reservoir operations model and power systems model allows one to first simulate reservoir operations and then optimize the dispatch of other power sources conditional on those outputs. However, optimizing reservoir operations to minimize fossil fuel emissions and maximize revenue requires a tight coupling between these two models in which outputs from the power systems model feed back to inform the reservoir operations model. In this case, a tight coupling is needed so that electricity prices and fossil fuels generation from the power systems model can inform the hydropower operations in the reservoir model.

We build such an integrated model using the Bonneville Power Administration (BPA) in the U.S. Pacific Northwest as a case study. BPA is a useful system for exploring the impacts of changing hydropower operations on electricity markets, as half of the region's electricity is generated by hydropower from 31 federal dams operated by BPA [36]. BPA's heavy dependence on hydropower exposes it to revenue fluctuations due to weather variability which, when combined with high fixed costs and obligations to meet minimum electricity delivery contracts, lead to financial losses. Though BPA has access to several risk mitigation tools, this financial risk has caught the attention of credit rating agencies who have cited hydrometeorological variability as a key factor in BPA's creditworthiness, and also led to a 2020 downgrade of BPA's rating by Moody's, a major rating company [37]. This financial risk highlights the need to assess reservoir operations in the CRB to stabilize BPA's revenues under variable hydrologic conditions. An integrated model of this system could also be used in future work to inform how BPA should adapt reservoir operations as their revenue is impacted by changes in the energy mix, climate change, and evolving regulations [38, 39].

The BPA system is also an interesting case study for understanding how hydropower operations can better complement renewables. Within the West Coast Power System, California has been rapidly expanding solar power capacity, while the Pacific Northwest has been expanding wind power capacity [40, 41]. When production of these renewables is high, reservoirs can hold back water and store it for subsequent production when renewable resource availability is low. Such load balancing is not restricted to the Mid-Columbia ("Mid-C"), market in which BPA resides, as BPA production can be exported to California as well. Coordinating power dispatch of renewables in this way could reduce the need to use fossil fuels for load balancing across the two regions, an environmental benefit of hydropower production that has not been quantified in prior

work.

In summary, this work fills two critical gaps in designing reservoir operations for conflicting social, economic, and environmental objectives: 1) it models the impact of changing hydropower operations on electricity prices to estimate (and ultimately, reduce) consequent impacts on revenue for power producers, and 2) it models the integrated dispatch of electricity generators to meet system demands across two interconnected balancing authorities, enabling coordinated operations for minimizing fossil fuel generation. These two objectives are included with traditional reservoir operating objectives of minimizing flooding and environmental flows violations. While the work focuses on operations within the Columbia River Basin, part of the Mid-C market, our approach to modeling integrated operations can be generalized to other systems, and we find generalizable insights on how to coordinate reservoir operations for these objectives that apply to hydropower systems around the globe.

2. Methods

2.1. California and West Coast Power System

This research aims to address the question of how power suppliers can adjust hydropower operations to minimize sustainability tradeoffs between reducing fossil fuel emissions and environmental flow violations, while maintaining or increasing hydropower revenue and flood protection. To investigate this question, we focus on the Columbia River Basin (CRB) in the Pacific Northwest (PNW) as a case study (Watershed 1 in Figure 1). In the CRB, there are 31 federal dams owned by the U.S. Army Corps of Engineers (USACE) and U.S. Bureau of Reclamation, which supply a significant portion (50-65%) of the region's electricity and offer 55.3 million acre-feet (AF) of storage for flood protection [3].

The USACE establishes operating guidelines for the dams to fulfill non-power objectives like flood control and environmental conservation. The Bonneville Power Administration (BPA) manages the dispatch of hydropower resources within these constraints. These decisions are influenced by market forces. The CRB dams are part of the Mid-Columbia (Mid-C) electricity market, where prices are affected not only by CRB reservoir operations but also by activities in the California Independent System Operator (CAISO) market [42].

Operating the CRB reservoirs within the USACE's established constraints is becoming increasingly challenging due to evolving political, environmental, and technological factors [43, 44, 45]. The widespread adoption of cost-effective renewable energy sources in the Western United States has negatively impacted BPA's revenue [46]. Nevertheless, there are opportunities to provide valuable generation flexibility to mitigate the variability of renewables. For instance, hydroelectric power in the CRB can be exported to California when its energy supply is insufficient. This influences electricity prices in both regions, affecting revenue for BPA, as well as consumer

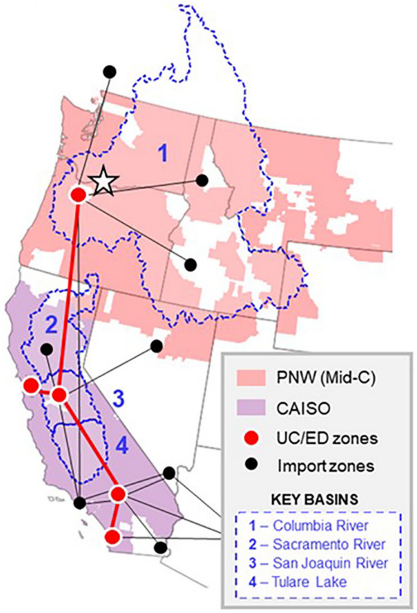

Figure 1. Map of the California and West Coast Power System modeled by CAPOW, reproduced from [38].

electricity costs.

However the optimal seasonality of hydropower operations can pose a threat to the survival of salmon and other fish that rely on natural flow patterns in the CRB [47]. Flood control along the Columbia River is another significant concern. In the CRB, this has historically been addressed by the Columbia River Treaty (CRT) under which Canada is required to operate their reservoirs within flood risk management guidelines. However, this treaty expires this year, after which the U.S. will need to make ad-hoc payments for continued flood protection until the treaty is renegotiated [48]. In the absence of a new treaty, the U.S. retains the right to request flood protection from Canada once its own reservoir capacity for flood risk management is exhausted, but these reservoirs may need to provide additional flood protection in the future should negotiations change the current agreement. These additional operational objectives for flood protection and environmental flows may limit the ability of hydropower to serve as a renewable energy source for load balancing.

In this study, we optimize operations at four of the BPA dams shown in Figure 2a: Hungry Horse (HGH), Libby (LIB), Dworshak (DWR) and Grand Coulee (GCL). While there are 31 federal dams, only six of them are storage dams, with the remainder operating as run-of-river at the daily time step. Of the six storage dams, we chose the prior four for optimization based on their turbine ratio (turbine capacity / average inflow), and flood storage capacity, measured in days of average flow. We included dams in our optimization if they have a turbine ratio greater than 2 (GCL and HGH), or more than 250 days of flood storage (HGH, LIB, and DWR). These thresholds were chosen to ensure that the selected reservoirs have significant capacities for either power generation

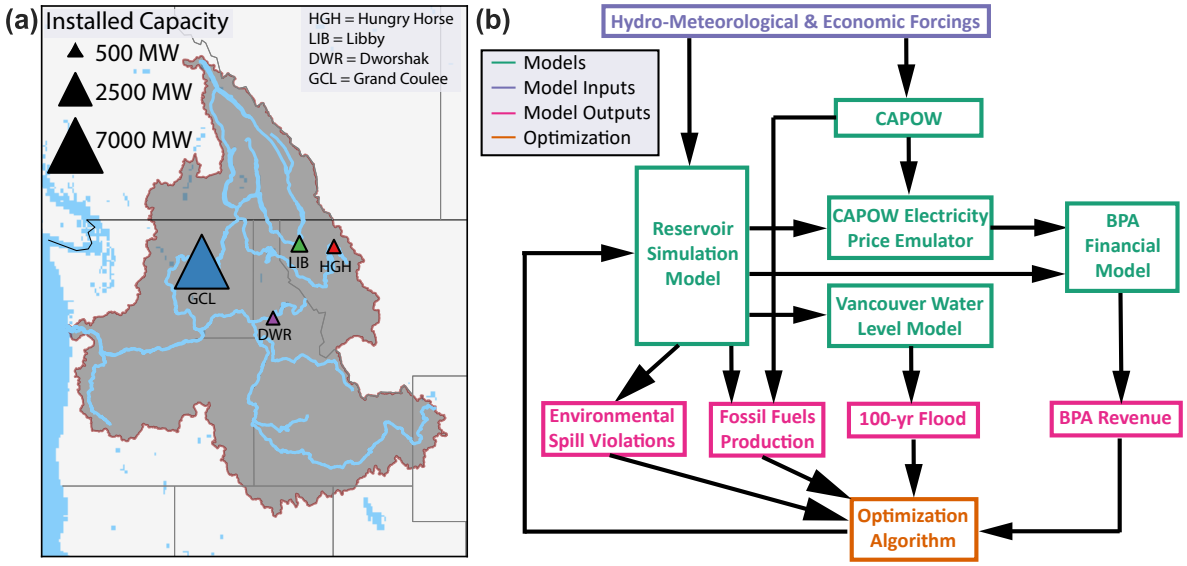

Figure 2. a) Map of the Columbia River Basin (CRB) and location of reservoirs whose operations we optimize. b) Integrated Reservoir System Management model (RSM), which consists of a reservoir simulation model of the CRB and an energy systems model of the California and West Coast Power System (CAPOW).

or flood mitigation. The storage and power capacities of these four reservoirs are listed in Table A1.

2.2. Integrated Water-Energy Model

In order to design better multi-objective hydropower operations at the four dams in Figure 2a, we need an integrated, tightly-coupled energy-water systems model. Figure 2b illustrates the components of this integrated model and their connections. Each model component is described in more detail within its own section.

For the reservoir system, we represent current operations in the CRB using a Python translation of the Hydro System Seasonal Regulation (HYSSR) model, originally written in Fortran [49]. This model is described in Section 2.3. We adapt the HYSSR model by converting it from a simulation model to an optimization model for stochastic optimization. The objectives under consideration are environmental (deviations from spills targets for salmon migration and fossil fuel generation), economic (BPA revenue), and social (flood protection). Environmental spills violations are calculated directly from the reservoir simulation model, while all other objectives require additional component models for their computation.

Environmental spills are calculated as the sum of squared deviations in spills simulated by HYSSR at seven reservoirs downstream of Grand Coulee from targets informed by personal communication with USACE ([50]; see Table A2 for the list of reservoirs under the spills violations constraint). Minimum spills during salmon migration to the Pacific Ocean allow juveniles to more easily travel downstream without

204 going through hydropower turbines, while maximum spills prevent dissolved gases from
205 exceeding 110-120% saturation, levels that can give the fish gas bubble disease [51]. The
206 flood objective is calculated using a statistical model of the water level in Vancouver,
207 WA as a function of discharges from the most downstream dam (Bonneville) and other
208 tidal components, with the goal of reducing peak levels (see Section 2.4).

209 Estimating BPA revenue and electricity generation from fossil fuels requires an
210 additional power dispatch model, described in Section 2.6. BPA revenue is calculated
211 as a function of the hydropower generation simulated by HYSSR and electricity prices.
212 Electricity prices are computed by integrating the HYSSR model with the California
213 and West Coast Power System model (CAPOW). CAPOW (described further in Section
214 2.5) is a unit commitment and economic dispatch model for electricity markets in
215 the Mid-Columbia and California Independent System Operator (CAISO) regions [52].
216 It represents all types of generators, including renewable and non-renewable sources,
217 and considers interactions with other regions in the Western Electricity Coordinating
218 Council. From this model, we can also determine how much hydropower generated in
219 Mid-C in excess of its demand can be exported to CA to reduce its fossil fuel generation.

220 The integrated Reservoir System Management model (RSM), as depicted in Figure
221 2b, takes as inputs historical or synthetic meteorological data and a reservoir control
222 sequence (to be optimized), and provides as outputs daily measures of renewable and
223 non-renewable electricity generation, electricity prices, flood levels, environmental spills,
224 and BPA revenue.

225 *2.3. Reservoir Simulation Model*

226 For the reservoir system, we represent current operations in the CRB using the Hydro
227 System Seasonal Regulation (HYSSR) model, an existing operations model for the
228 CRB developed by the U.S. Army Corps of Engineers for planning short and long-
229 range operations. HYSSR represents the 48 largest reservoirs in the CRB, with a total
230 installed hydroelectric capacity of 34 GW. Nine of the 48 dams (six in the U.S. and
231 three in Canada) impound storage reservoirs whose releases are governed by historical
232 nonlinear rules, while the remainder are considered run-of-river, i.e. their daily release
233 is the same as their daily inflow. These reservoirs contain numerous powerhouses and
234 turbines that need to be operated in a specific order based on seasonal requirements,
235 including fish passage and environmental constraints.

236 Hydropower generation by dams is calculated using the following equation, which
237 relates the physical properties of the water flow to electrical power output:

$$P = \eta \rho g h r^{PH} \tag{1}$$

238 where P represents the electrical power generated in watts (W), ρ is the density of water
239 (1000 kg/m^3), g is the acceleration due to gravity (9.81 m/s^2), h is the hydraulic head
240 (m), r^{PH} is the flow rate through the powerhouse in cubic meters per second (m^3/s),

and η is the coefficient of efficiency, a dimensionless factor that accounts for losses in the system.

To model oversupply events, which require a shorter time step, HYSSR has been adapted to daily operations. This modified version includes 46 dams, categorized as storage or run-of-river projects. Storage projects manage inflows for flood control, water supply, and power production, storing peak runoff from spring and summer for later release. Run-of-river projects pass inflows directly through turbines (and spills, if inflows exceed the turbine capacity).

The modified HYSSR model calculates daily storage, outflows, and power generation based on inflows, discharge requirements, storage levels (for storage projects), and operational rule curves. These rule curves consider projected inflows (here, using perfect forecasts), flood control, power needs, design limits, and regulatory constraints. Using synthetic streamflow data and rule curves, the model provides daily values for reservoir storage, outflow, and hydropower production. Generation from each of the unmodeled dams (totaling 12.5% of system hydropower capacity) is estimated by proportionally scaling generation from the closest modeled dam based on the ratio of their capacities [46].

Finally, in our optimization, we change the operations at four of the HYSSR dams, as described in Section 2.7.

2.4. Downstream water level model

In the CRB, the main location of concern for flood control is just above the confluence of the Columbia and Willamette Rivers in Vancouver, WA. Water levels in Vancouver, WA are mainly influenced by releases from the Bonneville Dam, tidal fluctuations, and backflow from the Willamette River. A statistical model was developed to estimate the water level at the gauge in Vancouver, WA utilizing discharges from the Bonneville Dam, periodic functions representing the tide, and prior model errors as predictors. Prior model errors capture persistence, including in influences from the Willamette. The model is specified as follows, with the flood level at time t, denoted as Y_t, calculated using the equation:

$$\begin{aligned}\log(Y_t) = \beta_0 + \beta_1 \cdot \log(\mathrm{r}_{BON,t}) + \beta_2 \cos\left(\frac{2\pi t}{365}\right) + \beta_3 \sin\left(\frac{2\pi t}{365}\right) \\ + \beta_4 \cos\left(\frac{2\pi t}{14.75}\right) + \beta_5 \sin\left(\frac{2\pi t}{14.75}\right) + w_t + \phi_1 w_{t-1} + \phi_2 w_{t-2},\end{aligned} \tag{2}$$

where, β_0 represents the intercept of the model, β_1 quantifies the impact of log-transformed discharge from the Bonneville Dam on flood levels, and β_2 and β_3 capture the seasonal effects within the year, β_4 and β_5 capture the tidal effects each month, w_t are residuals distributed as $w_t \sim \mathcal{N}(0, 0.094^2)$ and ϕ_1 and ϕ_2 are moving average coefficients on the past two time steps of residuals. The term $r_{BON,t}$ refers to the discharge from the

most downstream dam of our network Bonneville in thousands of cubic feet per second (kcfs). The values of the intercept and coefficients are reported in SI Table S5.

Due to a limited historical record of six years of daily water level data, the model was fit to the entire record rather than employing split training and testing. Over this period, the model exhibits strong predictive power, with an adjusted R^2 value of 0.82 (Figure 3). Additionally, the residuals of the model follow a normal distribution (see SI Figure S2), indicating that the model adequately captures the underlying patterns in the data. When simulating water levels in our model, we add randomly generated noise from this distribution to ensure we capture the full variance of downstream water levels and do not under-predict extremes.

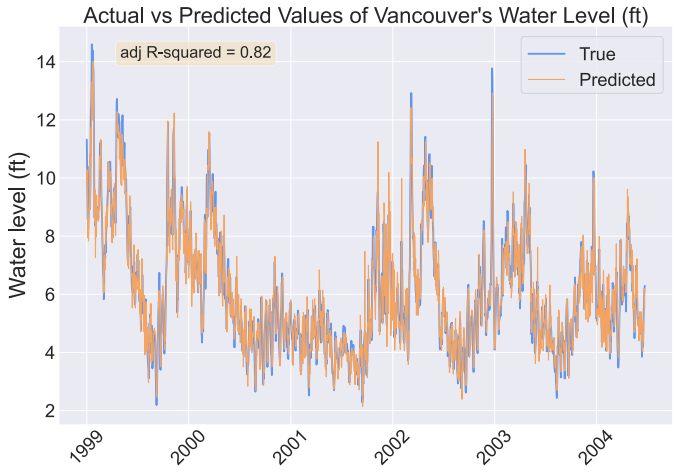

Figure 3. Actual vs predicted values of Vancouver's water level.

2.5. Energy Prices Model: CAPOW

The California and West Coast Power System Model (CAPOW) generates synthetic data of electricity demands and supply, and then uses a least-cost electricity dispatch model to calculate electricity prices in the California Independent System Operator (CAISO) and the informal Mid-Columbia (Mid-C) markets. It consists of two major components, "Stochastic Engine" and "Unit Commitment/Economic Dispatch (UC/ED)".

The stochastic engine uses a vector auto-regressive model to generate standardized anomalies of synthetic hydro-meteorological data including temperature, wind speed, and irradiance, that are then un-standardized based on monthly-varying estimates of each variable's mean and standard deviation. Synthetic "modified" streamflows are then generated from a fitted Gaussian copula, conditioned on the heating degree days from the synthetic hydro-meteorological data. Modified streamflows refer to naturalized, i.e. unregulated flows, minus evaporation and diversions. Thus, we do not make decisions around water supply diversions in our optimization model, which is reasonable given the limited ability to change them through the existing water rights system. The synthetically generated hydro-meteorological data is also used to simulate stochastic

electricity demands and supply through a number of regression models (see [52] for more details).

On the supply side, solar and wind capacity factors are simulated from multivariate regression models applied to the stochastically generated irradiance and wind speed data, respectively. Hydropower generation is estimated by simulating reservoir operations over the synthetically generated streamflow time series. Any simulated generation in excess of the synthetically generated demands is assumed to be curtailed. As discussed in Section 2.3, dams representing over 85% of hydropower capacity in the Pacific Northwest are modeled using a Python translation of the Hydro System Seasonal Regulation (HYSSR) model for the CRB. Dams on the Willamette River in the Pacific Northwest are simulated by a Python translation of a HEC-ResSim model. Finally, the Operation of Reservoirs in California model (ORCA; [53]) simulates hydropower generation in the major dams of California, which sums up to the total hydropower supply in the west coast [52].

In the UC/ED model, the dispatch of electric generators across the CAISO and Mid-C markets is meticulously determined using separate least-cost mixed integer linear programs for each region, tailored to meet the unique power demands of each system. The marginal cost of electricity from solar, wind, and hydropower is set to 0. As such, thermal generators like natural gas and coal are dispatched last. The market price is set by the cost of the most expensive electricity source once cheaper options are exhausted. The UC/ED model includes interconnections between the Mid-C and CAISO markets, so demands are met while accounting for imports and exports between the two regions, which are generated synthetically based on historical patterns and transmission capacity. The dispatch decisions are optimized for every hour over the next 48 hours using perfect foresight. However, decisions are only implemented for the first 24 hours, and then re-optimized for the next 48-hour window. This is performed over a 1-year horizon and run independently across 100 different years. For a comprehensive understanding of the methodologies originally employed in this study, readers are encouraged to consult the detailed exposition provided by [52], especially its Supplementary Information.

While CAPOW is powerful in enabling us to predict the market impacts of changing reservoir operations, it is too computationally expensive to couple with an optimization model. As such, we first ran CAPOW over 1000 years of synthetic hydro-meteorological data and then used those model runs to build statistical surrogates of electricity prices in the CAISO and Mid-C markets. The surrogate models are linear regression equations (equations 3-4) that predict daily prices in the two regions in \$/Mwh as a function of energy demands, exports, imports, solar, wind, and hydro generation:

$$\begin{aligned} Prices_t^{\text{MidC}} = \max\Big(&\beta_0 + \beta_1 \cdot Demands_t^{\text{MidC}} + \beta_2 \cdot Exports_t^{\text{MidC}} + \beta_3 \cdot Wind_t^{\text{MidC}} \\ &+ \beta_5 \cdot Hydro_t^{\text{MidC}} + \beta_6 \cdot Imports_t^{\text{MidC}} \\ &+ \beta_7 \cos\left(\frac{2\pi t}{365}\right) + \beta_8 \sin\left(\frac{2\pi t}{365}\right) + \epsilon_t^{\text{MidC}}, 10\Big) \end{aligned} \tag{3}$$

$$Prices_t^{\text{CAISO}} = \max\Big(\beta_0 + \beta_1 \cdot Demands_t^{\text{CAISO}} + \beta_2 \cdot Exports_t^{\text{CAISO}} + \beta_3 \cdot Solar_t^{\text{CAISO}} + \beta_4 \cdot Wind_t^{\text{CAISO}} + \beta_5 \cdot Hydro_t^{\text{CAISO}} + \beta_6 \cdot Imports_t^{\text{CAISO}} + \beta_7 \cos\left(\frac{2\pi t}{365}\right) + \beta_8 \sin\left(\frac{2\pi t}{365}\right) + \epsilon_t^{\text{CAISO}}, 10\Big). \tag{4}$$

The models were trained over 800 of the 1000 years and their performance was tested on the remaining 200 years. The values of all predictors are reported in SI Tables S3 and S4. Figure 5 shows the actual vs predicted values of the energy prices in the CAISO and informal Mid-C markets simulated by CAPOW vs. our emulator over the test set. The emulators in both the markets provide a good fit with adjusted R^2 values of 0.89 and 0.82 in CAISO and Mid-C, respectively. We reproduce remaining variability in our integrated model by adding bootstrapped residuals (ϵ_t^{MidC} and ϵ_t^{CAISO}) from the emulators to their predictions, conditioning the bootstrapping on the 10-percentile width bin in which the predictions lie, as in [54]. See SI Figure S3 shows the empirical cumulative distribution function of CAPOW prices vs. those simulated by our surrogates with added residual noise.

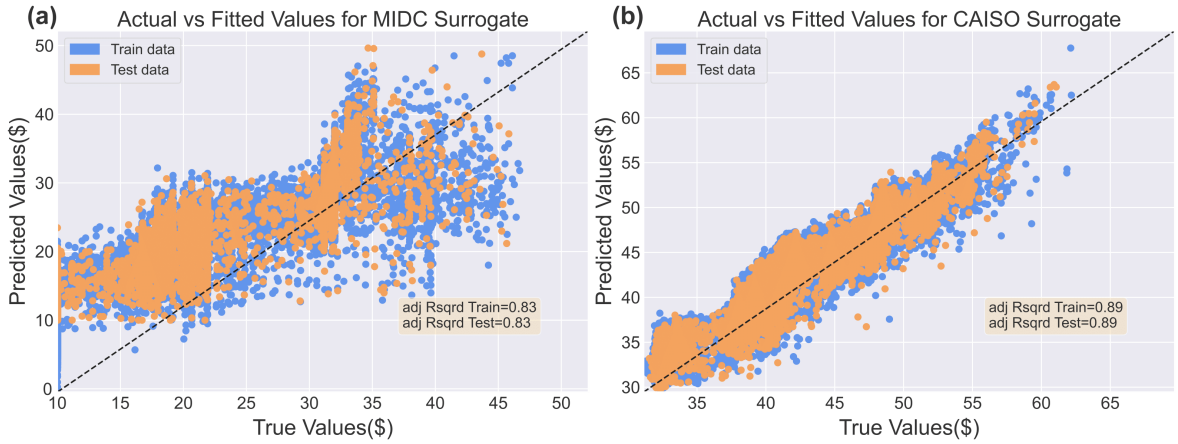

Figure 4. Actual vs predicted values of the statistical surrogates of the (a) Mid-C and (b) CAISO markets.

2.6. Bonneville Power Administration Financial Model

The Bonneville Power Administration (BPA) is a power marketer in the U.S. Pacific Northwest, responsible for selling the hydroelectricity generated at the 31 federal dams in the Federal Columbia River Power System (FCRPS). Because this hydropower contributes 80% of BPA's overall generation capacity [55], it is financially vulnerable to temperature and hydrologic variability, which influence electricity demand and generation, respectively. This vulnerability has been noted by credit rating agencies and internal reporting and has contributed to the depletion of BPA's line of credit with

the U.S. government, one of its three primary risk management tools [37, 56, 57, 58]. Prior analysis has suggested that an inability to mitigate its hydrometeorological risk could lead to losses of up to $200 million [59] and over $1 billion in costs [60].Adjusting the timing and volume of water releases and power generation can mitigate the impact of hydrometeorological variability, but influences other system objectives.

To account for the linkage between hydropower production and financial outcomes, this work uses the BPA financial model developed by [59] and refined by [60], which takes into account BPA's existing risk management tools (cash reserves, line of credit, and tariff adjustments). The model uses hydropower generation and downscaled demand from CAPOW as inputs. Revenue is calculated daily, largely from electricity sales to meet firm obligations at fixed prices. Surplus electricity is assumed to be sold directly on the wholesale Mid-C electricity market or exported to and sold within the CAISO market, depending on which market has higher prices. Should hydropower generation fall short of BPA's fixed electricity delivery obligations, BPA must purchase compensatory electricity to offset the deficit. In our model, this is either purchased from the Mid-C or imported from CAISO, whichever is cheaper. Annual net revenues are simulated by subtracting BPA's operating costs, held constant at 2018 historical values, as in [59].

2.7. Formulation of multi-objective optimization problem

2.7.1. Formulation of objectives and constraints In this study, we utilize Evolutionary Multi-Objective Policy Search (EMODPS; Giuliani et al. [16]) to find a set of non-dominated reservoir operating policies, p^*_θ, that minimize a vector of operating objectives $\bar{J}$:

$$p^*_\theta = \underset{p_\theta}{\text{argmin}} \quad \bar{J} \tag{5}$$

where

$$\bar{J} = |\, J^{env}\,,\, J^{fld}\,,\, -J^{rev}\,,\, J^{fos}\,|. \tag{6}$$

Each element of $\bar{J}$ is defined below, while the form of the operating policies p_θ is defined in Section 2.7.2. The outcome of the optimization is a set of non-dominated solutions, called the Pareto approximate set, in which no solution outperforms another on all objectives.

Environmental Spills. Let $spills_{i,t}$ represent the spills from reservoir i on day t, $\text{minSpill}_{i,t}$ be the minimum desired spills from reservoir i on day t to enable salmon migration through the dams, and $\text{maxSpill}_{i,t}$ be the maximum desired spills from reservoir i on day t to prevent supersaturation of dissolved gases above water quality standards. The environmental spills objective is then defined by Equation 7:

$$J^{env} = \frac{1}{N_d} \sum_{i=1}^{N_r} \sum_{t=1}^{N_d} \Big[\max\Big(0, spills_{i,t} - \text{maxSpill}_{i,t}\Big)^2 + \max\Big(0, \text{minSpill}_{i,t} - spills_{i,t}\Big)^2 \Big]. \tag{7}$$

where N_r is the number of reservoirs with spills regulations (see A2) and N_d is the number of days in the simulation.

Flood protection. The flood objective, to be minimized, is calculated as the maximum water level at Vancouver, WA, over the course of the simulation. This is defined by equation 8, where Z_t^V is the water level at Vancouver, WA at time t.

$$J^{\text{fld}} = \max_{t \in N_d} \quad Z_t^V \tag{8}$$

Fossil Fuel Generation. The fossil fuels objective, to be minimized, is calculated as the average daily fossil fuel generation across the Mid-C and CAISO markets over the simulation horizon. Letting ${Fossils_t}^{\text{MidC}}$ represent the fossil fuel generation in the Mid-C market on day t, and ${Fossils_t}^{\text{CAISO}}$ represent the fossil generation in the CAISO market on day t, this is calculated by equation 9:

$$J^{fos} = \frac{1}{N_d} \sum_{t=1}^{N_d} \Big[{Fossils_t}^{\text{MidC}} + {Fossils_t}^{\text{CAISO}} \Big] \tag{9}$$

where ${Fossils_t}^{\text{MidC}}$ and ${Fossils_t}^{\text{CAISO}}$ are calculated using algorithm 1, provided in the Appendix. This algorithm describes how hydropower generated by our optimized policies in excess of HYSSR generation is used to reduce fossil fuel generation in the two regions so that total power generation does not exceed total demand. Excess hydropower is first used to reduce Mid-C fossil fuel generation down to a fixed minimum for the region, capturing reserves. Any remaining excess hydropower is then exported to CAISO, where fossil fuel generation is reduced down to a separate region-specific minimum. If total generation still exceeds total demand, the remaining excess hydropower is curtailed. While this simplifies some elements of the power system, it greatly reduces the cost of re-running CAPOW with the alternative operating rules, while showing satisfactory performance in producing similar fossil fuel generation, as validated for one policy over three years in SI Figure S4.

BPA Revenue. The final objective is to maximize BPA's average annual net revenue in millions of U.S. dollars (USD), calculated by the BPA Financial Model:

$$J^{rev} = \frac{1}{N_y} \sum_{y=1}^{N_y} NR_y \tag{10}$$

where NR_y is BPA's revenue in million USD ($M) in year y and N_y is the number of simulated years.

Non-Zero Storage Constraint. Finally, we include one constraint in the model that storage cannot be negative at any of the reservoirs. While we also ensure this

through mass balance constraints in the simulation model, explicitly adding it as an optimization constraint prevented reservoirs from emptying during the time series used for optimization.

$$S_t^{res} \geq S_{min}^{res} \quad \forall \quad \text{res} \in \mathbf{RES} \tag{11}$$

where **RES** is the set of all model reservoirs and S_{min}^{res} is the minimum storage of reservoir res, $\forall \quad \text{res} \in \mathbf{RES}$

Note that for this study, we set S_{min}^{res} to zero for all the four reservoirs.

2.7.2. Formulation of operating policies In EMODPS, reservoir operating policies are parameterized within a certain family of functions describing the release from the reservoirs as a function of different state variables. We employ Gaussian Radial Basis Functions (RBFs) for these operating rules because Giuliani et al. [17] demonstrated their superior effectiveness in representing reservoir operating policies compared to Artificial Neural Networks (ANNs) with hyperbolic tangent activation functions. The RBF-based operating policies, described by equation 12, specify daily normalized releases from the k-th of K reservoirs at a given time t, denoted as u_t^k. These releases are determined as a function of B time-varying inputs, represented as v_t, also normalized within the range [0,1].

$$u_i^k = \sum_{i=1}^{N} w_i^k \exp\left(-\sum_{j=1}^{B} \frac{(v_{t,j} - c_{i,j})^2}{b_{i,j}^2}\right) \tag{12}$$

In this context, N represents the total count of RBFs and v_t is a vector comprising B inputs that have been scaled to fall within the [0,1] range. ($c_{i,j}$,$b_{i,j}$) represent the center and radius of the j-th input variable for the i-th RBF, and w_i^k signifies the weight associated with the i-th RBF for the k-th reservoir. The weights are constrained to add up to 1 for a given reservoir, k, representing a convex combination.

For the CRB system, we use $N = 8$ RBFs, $K = 4$ reservoirs, and $B = 7$ inputs, resulting in $N(2B + K) = 144$ optimized parameters. The seven RBF inputs are: the storage at each of the four reservoirs whose operations we optimize (see Table A1), the sum of interflows to the four reservoirs on the previous day and a cyclic representation of time captured by $\sin\left(\frac{2\pi t}{365}\right)$ and $\cos\left(\frac{2\pi t}{365}\right)$, all of which are normalized on $[0, 1]$. The sum of interflows can be thought of as unregulated inflows that would be received by the reservoirs in absence of operations. In the model, the true reservoir inflows are influenced by operations of upstream reservoirs, whose releases are either determined by the optimized RBF policies or modeled by HYSSR.

Finally, when simulating reservoir operations described by these rules, the normalized release is first un-normalized and then subjected to physical constraints to determine the true release. That is, if there is insufficient water to release what is prescribed, only the available water is released. Likewise, if only releasing what is prescribed would result in the reservoir exceeding its capacity, the excess is also released.

2.7.3. Multi-objective optimization algorithm In our research, we employ the Borg Multi-Objective Evolutionary Algorithm (MOEA; Hadka and Reed [61]) in conjunction with the EMODPS framework to identify the optimal set of operating policy parameters, denoted as θ. The Borg MOEA is particularly adept at handling complex multi-objective optimization problems, boasting features such as epsilon-dominance archiving, mechanisms to detect when the search is no longer making progress, randomized restarts to avoid being trapped in local optima, and the adaptive selection of search strategies. Its efficacy is well-documented, with performance that matches or exceeds other MOEAs across diverse problem scenarios, including reservoir operations [62].

For our computational needs, we utilized a multimaster parallelization of the Borg algorithm [63] using two masters. Optimization was performed on the University of Virginia's Rivanna High Performance Computing (HPC) cluster across 240 cores for a total Number of Function Evaluations (NFE) of 800,000 across the two masters. The total wall-clock time was 16 hours.

2.8. Performance evaluation

Reservoir operations were optimized over a simulation of 15 years of stochastic data generated by CAPOW. To evaluate the generalizability of the optimized operations, we resimulated the optimized rules over a 100-year out-of-sample data set.

3. Results and Discussion

3.1. Performance evaluation across objectives

We first explore the tradeoffs found by our optimized Pareto-approximate reservoir operating rules across the four system objectives. For reference, we compare these tradeoffs to the performance of existing operating rules, as modeled by HYSSR. The parallel axis plots in Figure 5 show this comparison over synthetic streamflows capturing historical hydrologic statistics. Figure 5a presents a set of 52 policies derived from the multi-objective optimization over the 15 years of synthetic flows to which they were optimized, while Figure 5b displays their performance on a separate validation set of 100 years of synthetic data. Each vertical axis in these plots represents performance for a specific objective, and each line represents a single policy, intersecting the axes at its objective values. The color of the line represents its performance on the fossil fuels objective, with dark blue indicating less emissions. The optimal direction on each axis is down. The performance of historical operating rules simulated by HYSSR is shown in black.

Figure 5a shows that over 90% of the optimized policies dominate HYSSR over the 15 years used in optimization, meaning they do better on all four objectives. While this decreases to 6% over the out-of-sample validation set of streamflows (Figure 5b), there clearly still exist better alternatives to balancing these system objectives. While we are able to find policies that dominate existing rules, there are still tradeoffs across

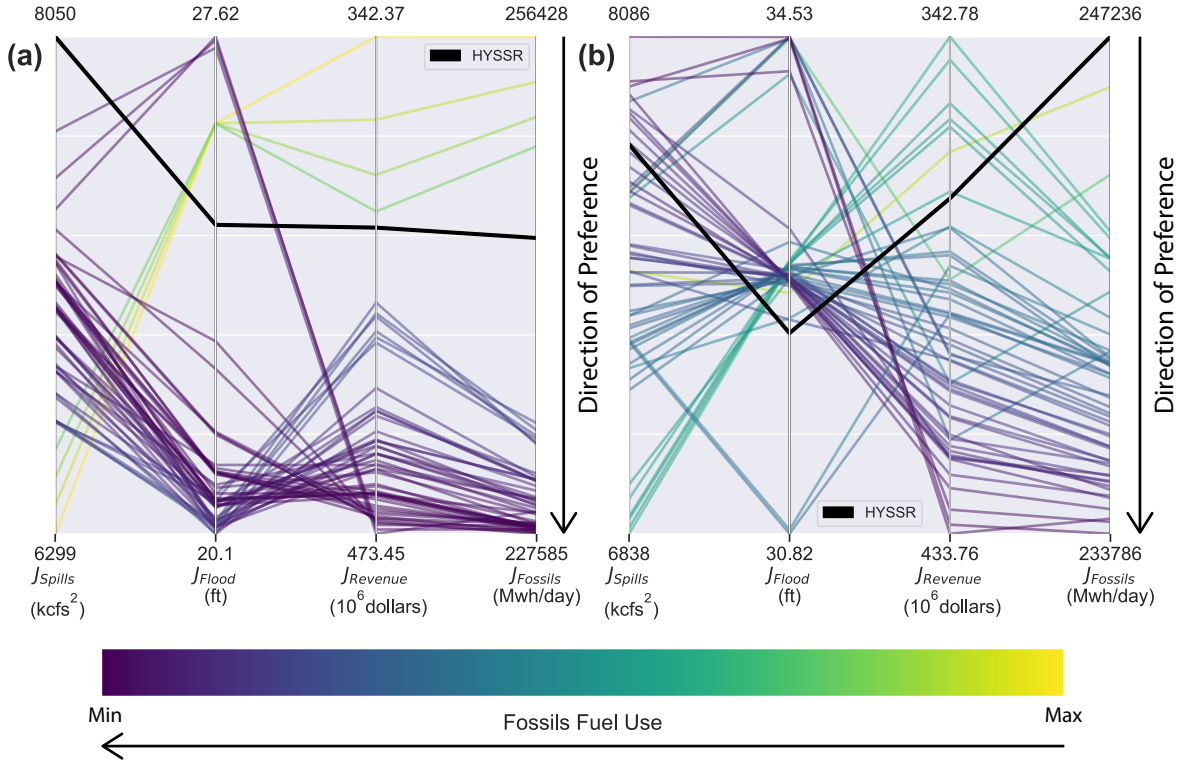

Figure 5. Policy performance of all optimized Pareto-approximate policies (colored lines) and HYSSR (black line) across (a) 15 years of synthetic flows used for optimization and (b) 100 years of synthetic flows used for validation.

the Pareto-approximate solutions. When lines cross between axes, it indicates tradeoffs between the objectives of those policies. tradeoffs also exist when colors swap orders between non-adjacent axes. This is clearly seen by the swapping colors between the fossil fuel use and flood objectives. This is because reducing fossil fuel use requires increased hydropower production, which in turn requires higher water storage levels in reservoirs for a greater head differential. However, keeping reservoirs full contradicts the flood protection objective, as it reduces the capacity to store floodwaters. We explore how such operating dynamics result in the observed tradeoffs in the following section.

3.2. Understanding water management tradeoffs

To understand how alternative operations result in the observed tradeoffs, we select the top four policies on each objective from the Pareto set, as well as HYSSR, for a more detailed analysis. The performance of these selected policies on the validation set of streamflows is illustrated in a parallel axis plot in Fig 6a, and the values of their objectives are given in Table A3. As noted before, a clear trade-off exists between fossil fuel reduction and flood protection, as evidenced by the fact that the best policy for fossil fuel reduction is the worst for flood protection. However, some objectives are positively correlated, such as fossil fuel use and BPA Revenue (Spearman rank coefficient=0.922),

since both are influenced primarily by hydropower production. As can be seen in the figure, these objectives have nearly overlapping best policies in the Pareto set. The environmental spills and flood protection objectives are also positively correlated (Spearman rank coefficient=0.331), as lower water storage in reservoirs reduces spills and increases capacity for floodwater storage. However, this correlation is not perfect, as can be seen by the stark performance differences of the best policies for Environmental Spills and Flood Protection across objectives.

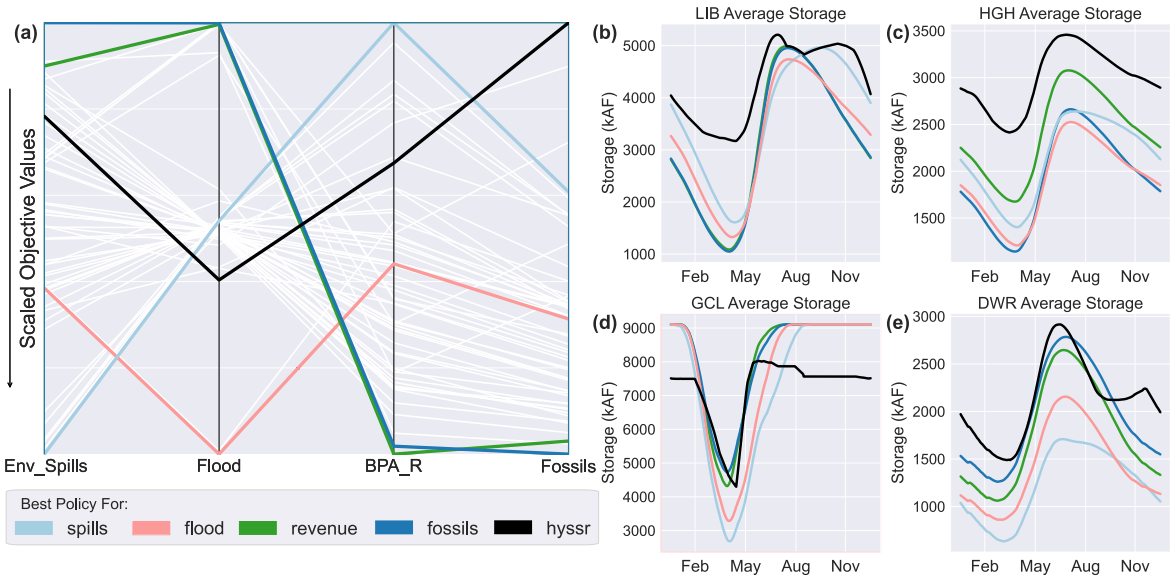

Figure 6. (a) Policies that perform best on each of the four objectives and HYSSR. (b-e) Average daily reservoir storage levels of the four optimized policies that are best on each objective and HYSSR at (b) Libby, (c), Hungry Horse, (d) Grand Coulee and (e) Dworshak.

Figure 6 also shows the average daily reservoir storage levels of each selected optimized policy and HYSSR in the four optimized reservoirs over the validation set of 100 years of synthetic streamflows. Analyzing average daily storage levels in these reservoirs reveals how varying operations help the select solutions achieve near-optimal outcomes for specific objectives. GCL, the largest hydropower dam in the U.S., is consistently operated at high storage levels across policies (Figure 6d). All policies decrease storage at GCL in advance of the spring snowmelt season, though, with those favoring flood protection and environmental spills drawing storage down more dramatically and refilling later. HYSSR maintains lower storage levels at GCL throughout the majority of the year. This requires less of a drawdown for flood protection in April, but still results in significantly inferior performance than all four policies on Fossil Fuel use and than all but the Best Spills policy on BPA Revenue.

Since the optimized policies prioritize hydropower generation at GCL to reduce fossil fuel use and maximize revenue, they compensate by utilizing the other three optimized reservoirs for flood protection. HYSSR, on the other hand, maintains

higher storage in the other reservoirs, resulting in worse performance on flooding and environmental spills than the policies favoring those objectives. HYSSR's backward coordination between GCL and the other reservoirs likely explains its inferior performance on all objectives compared to the Best Flood policy. HYSSR could clearly improve the coordination of its operations if even the policy that prioritizes flood protection maintains higher GCL storage.

It is clear from Figure 6 why the best policies for Fossil Fuel use and BPA Revenue do much better on these objectives and worse on Environmental Spills and Flooding than the other policies because of their higher storage at GCL (and DWR). However, it is not obvious from this figure why the Best Spills policy does so much worse than the Best Flood policy on the flood objective. To understand this, it is critical to note which reservoirs are subject to environmental spills regulations. Because fish migration does not occur upstream of the Mid-Columbia, dams above GCL (LIB and HGH) are not subject to these regulations. Table A2 lists all the reservoirs in the Mid-Columbia and Snake Rivers that have environmental spills regulations. Of these reservoirs, we only optimize operations at GCL as all others behave as run-of-river dams on the daily time step. Supplemental Figure S1a illustrates spills at GCL from the Best Spills and Best Flood policies, and Figure S1b the resulting water level in Vancouver. In this figure, it can be seen that the Best Spills policy has less spills at GCL than the Best Flood policy because its average storage is lower (as seen in Figure 6d), but the average storage of the other reservoirs, especially HGH (Figure 6c), is higher, leading to increased flood risk.

3.3. Understanding economic and environmental tradeoffs

The average storage levels shown in Figure 6 reveal useful insights into how alternative reservoirs in the CRB favor different water management objectives, but provide little insight into why they achieve their economic and environmental performance levels. However, unique to our integrated model of the reservoir-electricity-economic system, we can also derive insights into these tradeoffs by exploring how these average storage profiles influence spills and hydropower production, which in turn influence electricity prices and utility revenue.

We explore the complexity of economic and environmental tradeoffs by investigating the average annual time series of these variables in Figure 7. Here we see that, generally speaking, when hydropower production is high (Figure 7b), net sales are as well (Figure 7d), as surplus power can be sold on the market. Only in rare cases (Best Spills policy in summer) does the average hydropower production fall too far below demand such that even other PNW generators cannot meet demand, and BPA needs to purchase compensatory power on the market. While power sales generally corresponds to increased BPA revenue (Figure 7e), the relationship is somewhat muddied by the fact that electricity prices are generally inversely related to hydropower production (Figure 7c). The complex, nonlinear relationship between hydropower production and revenue

resulting from these competing influences on prices and sales are best understood by comparing the timing of generation across alternative policies.

In Figure 7b, it can be seen that HYSSR generates more hydropower than the other policies from June to August, a strategic approach to maximize power output during periods of higher water availability. This results in excess electricity that can be sold (Figure 7d), enhancing the utility's financial outcomes (Figure 7e), even if it decreases prices (Figure 7c). However, this is also a period of low demands which also leads to curtailment of other renewables. Our optimized operating policies instead distribute hydropower generation more evenly throughout the year, resulting in greater generation, sales, and revenue in the winter and fall. This explains how all of these policies achieve lower fossil fuel generation (see parallel axis plot in Figure 6a). For all but the Best Spills policy, this also results in greater revenue.

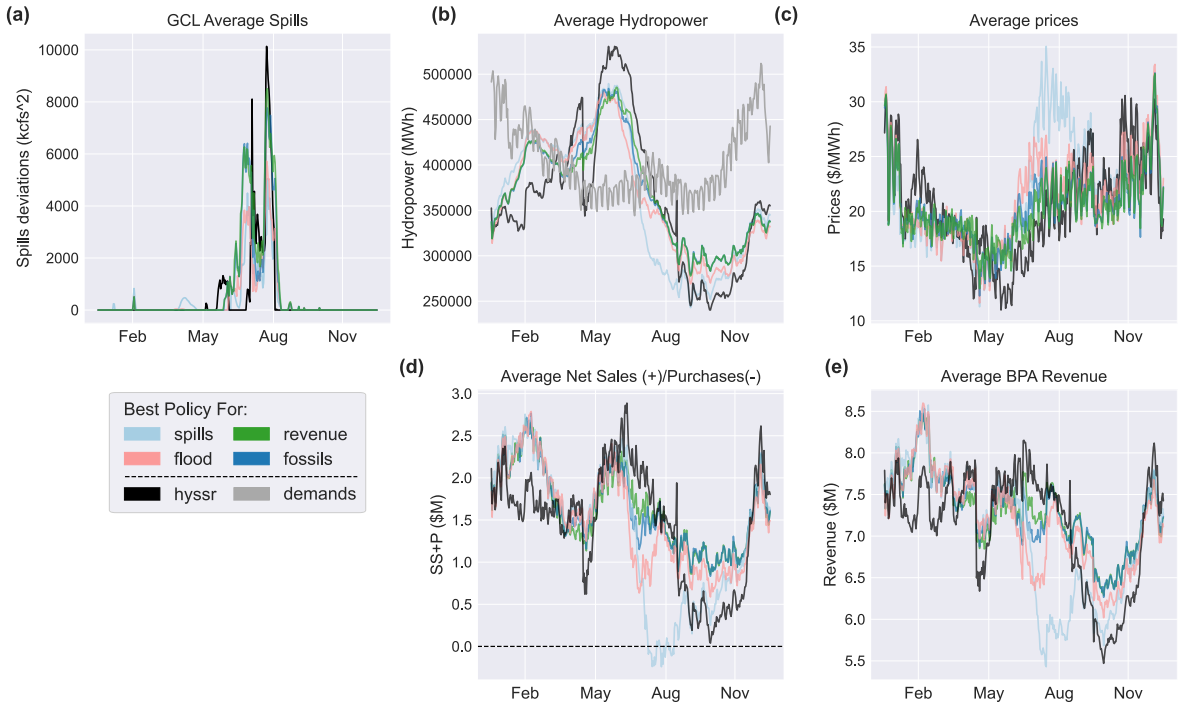

Figure 7. Average daily values of operational and economic variables over the year for the four selected policies and HYSSR. (a) Squared deviations from spills targets at Grand Coulee (kcfs^2); (b) Total Pacific Northwest (PNW) hydropower generation from each policy and PNW electricity demands (MWh); (c) Mid-Columbia electricity prices ($/MWh); (d) Net Sales ($> 0$) / Purchases ($< 0$) of electricity by the Bonneville Power Administration (BPA) ($M); (e) BPA Revenue ($M), representing economic returns from power transactions.

To understand why the Best Spills policy does not also increase revenue, we also plot the time series of average spills from GCL in Figure 7a. Across our Pareto front, we found that maximizing BPA revenue corresponds to increasing hydropower generation by maintaining high storage, increasing the probability of spills violations, while reducing fossil fuel use. However, the Best Spills policy achieves both lower spills and fossil

fuel emissions than HYSSR, but at a lower BPA revenue. Figure 7 reveals that this anomalous tradeoff is attributable to the timing of the releases, instead of simply the volumes released.

As can be seen in Figure 7a, the majority of spills at GCL from all policies occur during the late summer and early fall, specifically from June to mid-August. Crucially, July is a period of relative scarcity in renewable energy, as electricity demands begin to exceed hydropower supply (see Figure 7b). This is especially true for the Best Spills policy. The deficit in cheap renewable generation translates to an increase in Mid-C electricity prices during this period (Figure 7c), as more expensive thermal generators are activated to meet demand. Compounding the decrease in hydropower generation and corresponding sales, BPA must also continue to meet its fixed electricity delivery contracts and so is forced to purchase electricity at the high Mid-C price (Figure 7d). Consequently, although the spills-focused strategy may generate substantial hydropower at other times of the year, the reduced revenue and increased costs during this peak period illustrate a significant operational challenge that results in decreased BPA revenue. While HYSSR is able to generate greater hydropower during this period to reduce prices and increase revenue, shifting hydropower seasonality in this way comes at the expense of greater fossil fuels emissions over the course of the year.

This temporal misalignment underscores the need for strategically timed water releases to optimize both environmental and economic outcomes in hydropower operations. The Best Revenue and Best Fossil Fuels policies are able to better shift generation compared to HYSSR than the Best Spills policy so that reduced fossil fuel use does not come at the expense of decreased revenue. However, their greater hydropower production is still achieved by higher storage levels that result in greater environmental spills (Figure 7a). The Best Flood policy is able to strike the best balance. It refills GCL more slowly than all but the Best Spills policy (Figure 6d), resulting in less environmental spills violations than all but this policy as well. Yet its faster refill at GCL than the Best Spills policy avoids the spikes in electricity prices and need to buy power on the market at this price, ensuring its reduced fossil fuel use compared to HYSSR also results in greater BPA revenue.

3.4. Performance evaluation across hydrologic years

Figures 6-7 illustrate how select reservoir operating policies behave on average across years, highlighting the importance of properly timing releases to balance competing objectives. However, it also informative to understand how operations differ across years to manage inter-annual variability. To understand this, Figure 8 shows the behaviour of the Best Flood policy across 100 simulated years, not just on average. We select this policy since it outperforms HYSSR on all objectives. The blue shaded regions in Figure 8 indicate percentiles above the median, while the red regions indicate percentiles below the median. Black lines represent the minimum, median (dashed), and maximum values when simulating HYSSR operations over the same years.

From Figure 8, it is clear that the Best Flood policy makes use of the variables informing its releases (storage at the four reservoirs, their total inflow and day of the year) better than HYSSR. Figure 6 showed that on average, the Best Flood Policy is generally able to maintain higher storages at GCL and release more water for the hydropower objective. However, Figure 8c shows that in advance of the flood peak, it makes better use of information from the inflow state variable, drawing down more or less than HYSSR in advance of the peak based on what is needed to improve flood protection. Figure 6 showed these policies draw down GCL storage to similar levels on average during the spring, masking the greater variability in storage seen by the more dynamic Best Flood policy. While the Best Flood policy does occasionally empty the reservoir in the driest of the validation years, this should not be of practical concern due to its low frequency (once in 100 years), and it could potentially be avoided by applying a harsher minimum storage constraint during optimization (see Equation 11). Outside of the spring, the Best Flood policy refills GCL to higher levels than HYSSR that it maintains the rest of the year to improve hydropower production. Interestingly, this shift to higher storage levels applies to the whole storage distribution, with even the minimum optimized level exceeding the maximum HYSSR level, not just their respective mean levels, as seen in Figure 6.

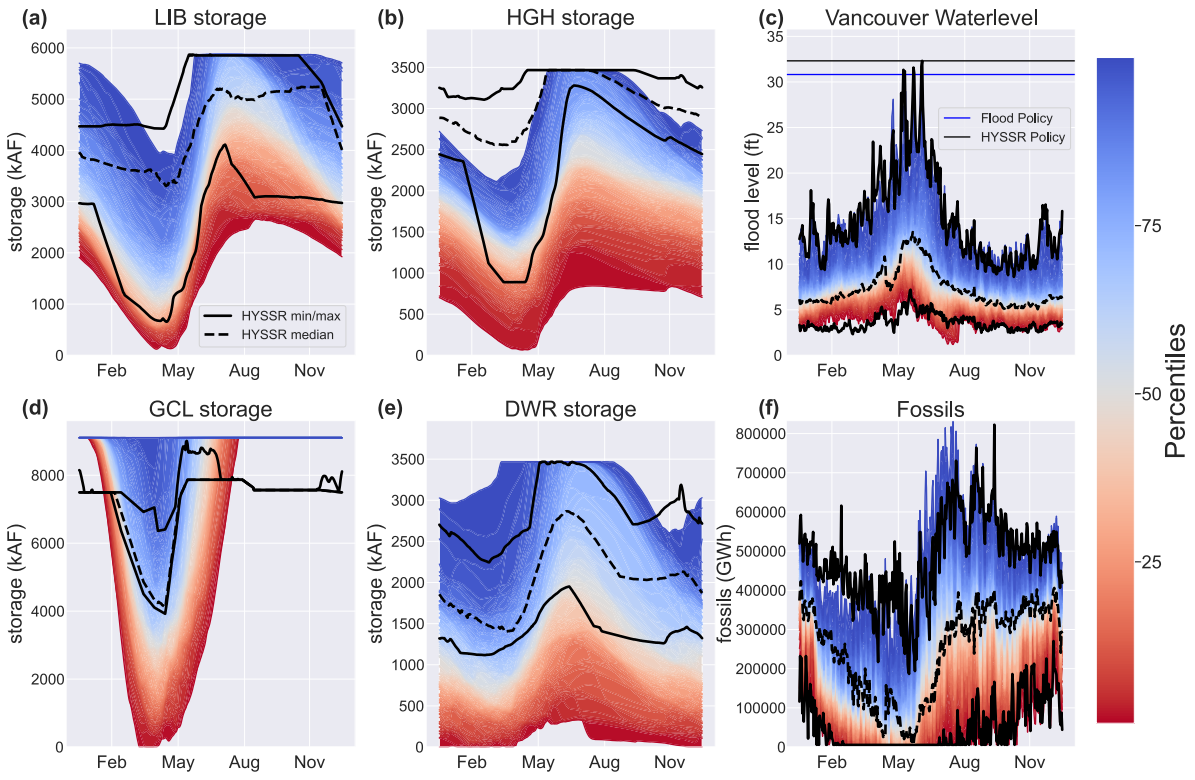

Figure 8. Storage percentiles of the Best Flood Policy at (a) Libby, (b) Hungry Horse, (d) Grand Coulee and (e) Dworshak across validation set of 100 synthetic years, as well as the corresponding percentiles of (c) the water level at Vancouver, WA and (f) Mid-C Fossil Fuels generation. Black lines represent the minimum, median (dashed), and maximum values simulated by HYSSR over the same 100 years.

Figure 8 also gives us some more insights into how the reservoirs coordinate amongst themselves in the network. As seen for the mean, in addition to keeping storage higher than HYSSR in GCL, the Best Flood policy generally keeps storage lower in HGH and DWR, as they have greater storage capacity but lower hydropower potential, making them better for flood protection. Storage in LIB is more similar on average, but again, the within-year distribution changes to maintain higher levels in all but the spring, when it draws down more in advance of the peak flow. Similar to GCL, we also see that the storage distribution of the optimized policy at DWR is generally more variable than for HYSSR, adapting its operations more in response to state information. Thus, the optimized policy represents a significant improvement over the historical operation rules (HYSSR) by more effectively using storage and inflow information to balance conflicting hydropower and flood protection objectives, improving performance on both.

The benefits of this improved coordination can be seen in Figures 8c and 8f showing the distribution of Vancouver water levels and total fossil fuel generation in Mid-C and CAISO. From January to late May, the median water level at Vancouver is similar for the Best Flood Policy and HYSSR. However, the greater drawdown at all reservoirs in April and May from the Best Flood policy reduces the median water level of this policy from the peak in June through the end of the summer in August, once all the reservoirs have refilled. This results in not only a lower median, but substantially lower peak as well (solid black and blue lines), shifting the whole distribution down during the summer.

At the same time, Figure 8f shows that the Best Flood policy effectively minimizes fossil fuel use as well. From late winter through early spring, the entire distribution of fossil fuel use reduces for this policy compared to HYSSR due to its elevated GCL storage that results in greater hydropower production that can be exported to California when it exceeds Mid-C demands. At the end of the spring, the reservoirs all have low storage and fossil fuel generation has to increase due to low hydropower production. However, this increase is seen by HYSSR as well, with the distributions of fossil fuel generation behaving very similarly for these to policies in the summer and fall. It is only during July-August at the highest percentiles that the Best Flood Policy sometimes requires greater fossil fuel use than HYSSR due to the hydropower generation falling short of demands, driven by lower inflows in those years. This sacrifice due to its greater storage variability across years is outweighed by its benefits in reducing fossil fuel use across all years in the months of February, March and April.

4. Discussion

The analyses above have illustrated many benefits to developing integrated models of the water, energy, and economic components of hydropower systems. First, such models enable an understanding of how changing hydropower operations impact objectives across all these areas. This can reveal interesting insights, which may include both unforeseen conflicts and unexpected synergies. For example, here we observed

unforeseen conflicts in reducing fossil fuel use vs. increasing revenue when moving from HYSSR to the Best Spills policy because of changes in the seasonality of releases. However, we also saw unexpected synergies in reducing environmental spills and fossil fuel emissions while increasing revenue when moving from HYSSR to the Best Flood policy. This was illustrated to be a byproduct of better coordination across reservoirs.

These insights were not only revealed because of the integrated model but through multi-objective optimization. A chief benefit of multi-objective optimization is that many non-dominated policies can be presented to stakeholders who can then deliberate with one another to arrive at an effective compromise solution. This *a posteriori* deliberation is valuable [64], as stakeholders often select a different policy from a non-dominated set than what their preferences solicited before optimization would imply [65]. Knowing this, we do not recommend any particular policy in this study, but highlight some of the benefits and drawbacks of different alternatives that could help inform that choice.

A stronger grasp of potential tradeoffs between competing objectives can also elucidate incentives or regulations that could be used to produce more desirable outcomes. For example, the objectives used in this model are tied to the river ecosystem (spills), BPA (revenues), households vulnerable to flooding (flood), and the broader public (fossil fuels). To incentivize BPA to reduce system-wide fossil fuel emissions, carbon credits could be granted for reductions enabled by switching operations. To incentivize BPA to reduce environmental spills, stronger regulations or penalties could be imposed. Indeed, this leaves room for additional work exploring how regulations interact across scales and governance levels. As Kosnik [66] notes, excessive regulation can lead to the "Tragedy of the Anticommons," whereby excessive regulation leads to sub-optimal usage. Combining integrated modelling with multi-objective optimization can help determine effective levels of regulations to mitigate these impacts, hopefully leading to improved water resource management.

5. Conclusions

This study uses the multi-reservoir Columbia River system in the U.S. Pacific Northwest to demonstrate the power of integrated water-energy models in deriving insights into how to best balance competing socio-economic and environmental objectives. Such insights can be gleaned through multi-objective optimization of alternative reservoir operating rules for balancing these objectives. Insights from our multi-objective optimization of the Columbia reservoir system include:

- producing non-dominated policies that can perform as well or better than the current reservoir operations across all economic, environmental, flood protection and fossil fuels objectives;
- more effectively using storage and inflow information to coordinate reservoir operations for conflicting hydropower and flood protection objectives across wet vs. dry hydrologic years, improving performance on both;

- highlighting the importance of strategically timed water releases in hydropower operations to balance the tradeoffs between environmental management and economic performance, especially during periods of renewable scarcity when demand can outpace hydropower supply, impacting both revenue generation and fossil fuel consumption.

While these findings are useful for informing how to adapt reservoir operations, many facets of the system are likely to change in the near future. As such, future work should consider how such factors might influence conclusions about how to best adapt operations. For example, it will be critical to understand how shifting weather patterns and water availability under climate change could impact reservoir operations and hydropower efficiency. Moreover, different technological development pathways, including the adoption of a broader mix of renewable energy sources in the energy landscape, may significantly influence what operations are most effective. Integrating these factors into the design of reservoir operations may reveal synergies or tradeoffs between hydropower and other renewables. Understanding these impacts will enhance our ability to reduce fossil fuel dependence and support sustainable energy production more effectively.

Appendix A. Additional tables

Table A1. Reservoirs under optimization

Reservoirs	Abbreviations	Storage Capacity (kAF)	Power Capacity (MW)
`Grand Coulee`	GCL	9107.2	6809
`Dworshak`	DWR	3468.0	400
`Hungry Horse`	HGH	3467.0	428
`Libby`	LIB	5870.0	600

Table A2. Reservoirs with environmental spills regulations

Reservoir	Abbreviation
`Grand Coulee`	GCL
`Chief Joseph`	CHJ
`Lower Granite`	LWG
`Little Goose`	LGS
`Lower Monumental`	LMN
`Ice Harbour`	IHR
`Bonneville`	BON

Table A3. Objective values of select policies

Selected Policy	Environmental Spills Violations ($kcfs^2$)	Max Flood Level (ft)	BPA Revenue ($M/year)	Fossil Fuels Generation (GWh/year)
Lowest Peak Flood	7,319	30.8	394	238.0
Least Spills	6,839	32.8	343	242.0
Highest Revenue	7,961	34.5	434	234.2
Lowest Fossil Fuels	8,086	34.5	432	233.8
HYSSR	7,816	32.3	372	247.2

Algorithm 1 Pseudocode for Energy-mix curtailment

for each timestep t **do**
  $U_t \leftarrow$ Hydro from the RBF releases
  $Hydro_t^{\text{MidC}} \leftarrow$ Hydro from HYSSR
  $Fossils_t^{\text{MidC}} \leftarrow$ Initial fossils in the Mid-C
  $Exports_t^{\text{MidC}} \leftarrow$ Initial energy exports in the Mid-C
  $Fossils_t^{\text{CAISO}} \leftarrow$ Initial fossils in the CAISO
  $Imports_t^{\text{CAISO}} \leftarrow$ Initial energy imports in the CAISO
  if $U_t = Hydro_t^{\text{MidC}}$ **then**
    $difference \leftarrow Hydro_t^{\text{MidC}} - U_t$
    $Fossils_t^{\text{MidC}} \leftarrow Fossils_t^{\text{MidC}} - difference$
  else
    $difference \leftarrow U_t - Hydro_t^{\text{MidC}}$
    $Fossils_t^{\text{MidC}} \leftarrow Fossils_t^{\text{MidC}} - difference$
    if $Fossils_t^{\text{MidC}} \leq min\_fossils\_constraint$ **then**
      $ca\_exports\_diff \leftarrow min\_fossils\_constraint - Fossils_t^{\text{MidC}}$
      $Fossils_t^{\text{MidC}} \leftarrow min\_fossils\_constraint$
      $ca\_exports\_diff \leftarrow \max(ca\_exports\_diff, max\_exports\_constraint)$
      $Exports_t^{\text{MidC}} \leftarrow Exports_t^{\text{MidC}} + ca\_exports\_diff$
      $Imports_t^{\text{CAISO}} \leftarrow Imports_t^{\text{CAISO}} + ca\_exports\_diff$
      $Fossils_t^{\text{CAISO}} \leftarrow Fossils_t^{\text{CAISO}} - ca\_exports\_diff$
      if $Fossils_t^{\text{CAISO}} \leq 0$ **then**
        $hydro\_curt \leftarrow -(Fossils_t^{\text{CAISO}})$
        $U_t \leftarrow U_t - hydro\_curt$
        $Exports_t^{\text{MidC}} \leftarrow Exports_t^{\text{MidC}} - hydro\_curt$
        $Imports_t^{\text{CAISO}} \leftarrow Imports_t^{\text{CAISO}} - hydro\_curt$
        $Fossils_t^{\text{CAISO}} \leftarrow 0$
      end if
    end if
  end if
end for

Acknowledgements

This work was supported by funding from the University of Virginia School of Engineering and Applied Science. The authors acknowledge Research Computing at The University of Virginia for providing computational resources and technical support that have contributed to the results reported within this publication (`https://rc.virginia.edu`). The authors would also like to thank Prof. Jonathan Lamontagne, Tufts University and Steve Barton, Chief, Columbia Basin Water Management Division, USACE for helpful discussions on model development. Any opinions, findings, and

conclusions or recommendations expressed in this material are those of the author(s) and do not necessarily reflect the views of the funding entities.

Data Availability Statement

All code for this project is available in online repositories. The code for CAPOW is available at `https://github.com/romulus97/CAPOW_PY36`. All other model code can be found at: `https://github.com/samarthsing/CRB_reservoirs_optimization`. All data files are available at `https://doi.org/10.5281/zenodo.11962296`.

References

[1] Neil E Ward and David L Ward. Resident fish in the Columbia River basin: Restoration, enhancement, and mitigation for losses associated with hydroelectric development and operations. *Fisheries*, 29(3):10–18, 2004.

[2] US EPA. Columbia River Basin: State of the river report for toxics, 2009. Available Online: `https://www.epa.gov/columbiariver/2009-state-river-report-toxics`.

[3] BPA, USBR, and USACE. The Columbia River System Inside Story, Second Edition. Technical report, Federal Columbia River Power System, 2001. Available Online: `https://www.bpa.gov/-/media/Aep/power/hydropower-data-studies/columbia_river_inside_story.pdf`.

[4] Eric A. Stene. The Central Valley Project - Introduction, 2015. Available Online: `ttps://www.usbr.gov/history/cvpintro.html`.

[5] William L Graf. Dam nation: A geographic census of american dams and their large-scale hydrologic impacts. *Water resources research*, 35(4):1305–1311, 1999.

[6] Kaveh Madani and Jay R. Lund. Modeling approaches for sustainable reservoir management: A review. *Environmental Modelling & Software*, 25(12):1702–1715, 2010.

[7] Sebastián Vicuña and John A. Dracup. Climate change impacts on streamflow timing in the sierra nevada in california: implications for water resources management. *Hydrological Processes*, 22(7):906–918, 2008.

[8] Daniel P. Loucks and Eelco van Beek. Water resource systems planning and management: An introduction to methods, models, and applications. *Springer*, 2005.

[9] Matteo Giuliani, Andrea Castelletti, Roman Fedorov, and Piero Fraternali. A decision support system for real-time hydropower scheduling in a complex alpine river basin. *Environmental Modelling & Software*, 84:58–75, 2016.

[10] Thomas B Wild, Patrick M Reed, Daniel P Loucks, Martin Mallen-Cooper, and Erland D Jensen. Balancing hydropower development and ecological impacts in the

mekong: Tradeoffs for sambor mega dam. *Journal of Water Resources Planning and Management*, 145(2):05018019, 2019.

[11] Caroline C Arantes, Daniel B Fitzgerald, David J Hoeinghaus, and Kirk O Winemiller. Impacts of hydroelectric dams on fishes and fisheries in tropical rivers through the lens of functional traits. *Current Opinion in Environmental Sustainability*, 37:28–40, 2019.

[12] Margaret Palmer and Albert Ruhi. Linkages between flow regime, biota, and ecosystem processes: Implications for river restoration. *Science*, 365(6459): eaaw2087, 2019.

[13] M Giuliani, JR Lamontagne, PM Reed, and A Castelletti. A state-of-the-art review of optimal reservoir control for managing conflicting demands in a changing world. *Water Resources Research*, 57(12):e2021WR029927, 2021.

[14] Andrea Castelletti, Francesca Pianosi, and Rodolfo Soncini-Sessa. Water reservoir control under economic, social and environmental constraints. *Automatica*, 44(6): 1595–1607, 2008.

[15] John W Labadie. Optimal operation of multireservoir systems: State-of-the-art review. *Journal of water resources planning and management*, 130(2):93–111, 2004.

[16] Matteo Giuliani, Andrea Castelletti, Francesca Pianosi, Emanuele Mason, and Patrick M Reed. Curses, tradeoffs, and scalable management: Advancing evolutionary multiobjective direct policy search to improve water reservoir operations. *Journal of Water Resources Planning and Management*, page 04015050, 2016.

[17] M Giuliani, F Pianosi, and A Castelletti. Making the most of data: an information selection and assessment framework to improve water systems operations. *Water Resources Research*, 51(11):9073–9093, 2015.

[18] Afua Owusu, Jazmin Zatarain Salazar, Marloes Mul, Pieter van der Zaag, and Jill Slinger. Quantifying the trade-offs in re-operating dams for the environment in the lower volta river. *Hydrology and Earth System Sciences Discussions*, 2022:1–27, 2022.

[19] F Bertoni, A Castelletti, M Giuliani, and PM Reed. Discovering dependencies, trade-offs, and robustness in joint dam design and operation: An ex-post assessment of the kariba dam. *Earth's Future*, 7(12):1367–1390, 2019.

[20] Jazmin Zatarain Salazar, Patrick M Reed, Julianne D Quinn, Matteo Giuliani, and Andrea Castelletti. Balancing exploration, uncertainty and computational demands in many objective reservoir optimization. *Advances in water resources*, 109:196–210, 2017.

[21] Julianne D Quinn, Patrick M Reed, M Giuliani, and Andrea Castelletti. Rival framings: A framework for discovering how problem formulation uncertainties shape risk management trade-offs in water resources systems. *Water Resources Research*, 53(8):7208–7233, 2017.

[22] Julianne D Quinn, Patrick M Reed, Matteo Giuliani, Andrea Castelletti, Jared W Oyler, and Robert E Nicholas. Exploring how changing monsoonal dynamics and human pressures challenge multireservoir management for flood protection, hydropower production, and agricultural water supply. *Water Resources Research*, 54(7):4638–4662, 2018.

[23] Muhammad Usman Rashid, Irfan Abid, and Abid Latif. Optimization of hydropower and related benefits through cascade reservoirs for sustainable economic growth. *Renewable Energy*, 185:241–254, 2022.

[24] Maria D Bejarano, A Sordo-Ward, Iván Gabriel-Martin, and Luis Garrote. Tradeoff between economic and environmental costs and benefits of hydropower production at run-of-river-diversion schemes under different environmental flows scenarios. *Journal of Hydrology*, 572:790–804, 2019.

[25] Marta Zaniolo, Matteo Giuliani, Amare Bantider, and Andrea Castelletti. Hydropower development: Economic and environmental benefits and risks. In *The Omo-Turkana Basin*, pages 37–57. Routledge, 2021.

[26] Nicolò Stevanato, Matteo V Rocco, Matteo Giuliani, Andrea Castelletti, and Emanuela Colombo. Advancing the representation of reservoir hydropower in energy systems modelling: The case of zambesi river basin. *Plos one*, 16(12): e0259876, 2021.

[27] Abdus Samad Azad, Md Shokor A Rahaman, Junzo Watada, Pandian Vasant, and Jose Antonio Gamez Vintaned. Optimization of the hydropower energy generation using meta-heuristic approaches: A review. *Energy Reports*, 6:2230–2248, 2020.

[28] Yoan Villeneuve, Sara Séguin, and Abdellah Chehri. Ai-based scheduling models, optimization, and prediction for hydropower generation: Opportunities, issues, and future directions. *Energies*, 16(8):3335, 2023.

[29] Ioannis Kougias, Sandor Szabo, Fabio Monforti-Ferrario, Thomas Huld, and Katalin Bódis. A methodology for optimization of the complementarity between small-hydropower plants and solar pv systems. *Renewable Energy*, 87:1023–1030, 2016.

[30] Michelle TH Van Vliet, John R Yearsley, Fulco Ludwig, Stefan Vögele, Dennis P Lettenmaier, and Pavel Kabat. Vulnerability of us and european electricity supply to climate change. *Nature Climate Change*, 2(9):676–681, 2012.

[31] Camila Ochoa and Ann van Ackere. Winners and losers of market coupling. *Energy*, 80:522–534, 2015.

[32] Johannes Schmidt, Rafael Cancella, and Amaro O Pereira Jr. An optimal mix of solar pv, wind and hydro power for a low-carbon electricity supply in brazil. *Renewable Energy*, 85:137–147, 2016.

[33] MPNCR Kelman, M Pereira, and N Campodónico. Long-term hydro scheduling based on stochastic models. *EPSOM*, 98:23–25, 1998.

[34] B Bezerra, LA Barroso, R Kelman, B Flach, ML Latorre, N Campodonico, and M Pereira. Integrated electricity–gas operations planning in long-term hydroscheduling based on stochastic models. In *Handbook of Power Systems I*, pages 149–175. Springer, 2010.

[35] Alexandre Street, Davi Valladao, André Lawson, and Alexandre Velloso. Assessing the cost of the hazard-decision simplification in multistage stochastic hydrothermal scheduling. *Applied Energy*, 280:115939, 2020.

[36] Northwest Power and Conservation Council. Pacific northwest hydropower for the 21st century power grid, 2019. Available Online: `https://www.nwcouncil.org/energy/energy-topics/hydropower/`.

[37] Moody's. Rating action: Moody's downgrades BPA (OR) to AA2 from AA1; assigns AA2 rating to Morrow (Port of) OR's transmission revenue bonds; outlook is stable. `https://www.moodys.com/research/Moodys-downgrades-BPA-OR-to-Aa2-from-Aa1-assigns-Aa2--PR_906313039`, 2020. Accessed: 2021-11-01.

[38] Joy Hill, Jordan Kern, David E Rupp, Nathalie Voisin, and Gregory Characklis. The effects of climate change on interregional electricity market dynamics on the US West Coast. *Earth's Future*, 9(12):e2021EF002400, 2021.

[39] Jacob Wessel, Jordan D Kern, Nathalie Voisin, Konstantinos Oikonomou, and Jannik Haas. Technology pathways could help drive the US West Coast grid's exposure to hydrometeorological uncertainty. *Earth's Future*, 10(1): e2021EF002187, 2022.

[40] Anne Fischer. California solar generation grew twentyfold in a decade. PV Magazine USA, 2023. Available online: `https://www.pv-magazine-usa.com/2023/08/21/california-solar-generation-grew-twentyfold-in-a-decade/`.

[41] California Energy Commission. Data show clean power increasing, fossil fuel decreasing in california. *California Energy Commission*, 2023. Available online: `https://www.energy.ca.gov/news/2023-08/data-show-clean-power-increasing-fossil-fuel-decreasing-california`.

[42] Yufei Su, Jordan D Kern, Patrick M Reed, and Gregory W Characklis. Compound hydrometeorological extremes across multiple timescales drive volatility in california electricity market prices and emissions. *Applied Energy*, 276:115541, 2020.

[43] Asphota Wasti, Patrick Ray, Sungwook Wi, Christine Folch, María Ubierna, and Pravin Karki. Climate change and the hydropower sector: A global review. *Wiley Interdisciplinary Reviews: Climate Change*, 13(2):e757, 2022.

[44] WN Beer and JJ Anderson. Sensitivity of juvenile salmonid growth to future climate trends. *River Research and Applications*, 27(5):663–669, 2011.

[45] Larry Hittle, Steve Larson, Nancy Randall, and Preston Michie. Pacific northwest power generation, multi-purpose use of the columbia river, and regional energy legislation: An overview. *Envtl. L.*, 10:235, 1979.

[46] Yufei Su, Jordan D Kern, and Gregory W Characklis. The impact of wind power growth and hydrological uncertainty on financial losses from oversupply events in hydropower-dominated systems. *Applied energy*, 194:172–183, 2017.

[47] Emilie Person. Impact of hydropeaking on fish and their habitat. Technical report, EPFL-LCH, 2013.

[48] BPA. BPA 2018-2023 Strategic Plan. Strategic Plan DOE/BP-4808, Bonneville Power Adminsitration, Portland, Oregon, January 2018. Available Online: `https://www.bpa.gov/StrategicPlan/StrategicPlan/2018-Strategic-Plan.pdf`.

[49] United States Bonneville Power Administration, United States Army Corps of Engineers, and United States. Bureau of Reclamation. Modeling the System: How Computers are Used in Columbia River Planning. Technical report, 10 1992. Available online: `https://www.osti.gov/biblio/6575752`.

[50] Sue Nee Tan. *Computationally Efficient Hydropower Operations Optimization for Large Cascaded Hydropower Systems Reflecting Market Power, Fish Constraints, Multi-Turbine Powerhouses, and Renewable Resource Integration.* PhD thesis, Cornell University, 2017.

[51] Kathy E McGrath, Earl Dawley, and David R Geist. Total dissolved gas effects on fishes of the lower columbia river. Technical report, Pacific Northwest National Lab.(PNNL), Richland, WA (United States), 2006.

[52] Yufei Su, Jordan D Kern, Simona Denaro, Joy Hill, Patrick Reed, Yina Sun, Jon Cohen, and Gregory W Characklis. An open source model for quantifying risks in bulk electric power systems from spatially and temporally correlated hydrometeorological processes. *Environmental Modelling & Software*, 126:104667, 2020.

[53] Jonathan S Cohen, Harrison B Zeff, and Jonathan D Herman. Adaptation of multiobjective reservoir operations to snowpack decline in the western united states. *Journal of Water Resources Planning and Management*, 146(12):04020091, 2020.

[54] Farmer William H. and Vogel Richard M. On the deterministic and stochastic use of hydrologic models. *Water Resources Research*, 52(7):5619–5633, June 2016. ISSN 0043-1397. doi: 10.1002/2016WR019129. URL `https://agupubs.onlinelibrary.wiley.com/doi/abs/10.1002/2016WR019129`.

[55] Bonneville Power Administration. Hydropower impact. Bonneville Power Administration, 2024. Available online: `https://www.bpa.gov/energy-and-services/power/hydropower-impact`.

[56] Moody's. Credit opinion: Bonneville power administration, or update to discussion of key credit factors. `https://www.bpa.gov/Finance/FinancialInformation/Debt/BondInformation/Moodys%20Full%20Report%20May%202021.pdf`, 2021. Accessed: 2021-11-01.

[57] Standard and Poor's Global Ratings. Bonneville Power Administration, Oregon; Wholesale Electric. `https://www.bpa.gov/Finance/FinancialInformation/`

Debt/BondInformation/SP%20Full%20Report%20May%202021.pdf, 2021. Accessed: 2021-11-01.

[58] Fitch Ratings. Fitch rates Energy Northwest, WA Elec Rev Ref Bonds 'AA'; affirms Bonneville's IDR at 'AA' Fitch ratings (May). https://www.fitchratings.com/research/us-public-finance/fitch-rates-energy-northwest-wa-elec-rev-ref-bonds-aa-affirms-bonneville-idr-at-aa-04-05-2021, 2021. Accessed: 2021-11-01.

[59] Simona Denaro, Rosa I Cuppari, Jordan D Kern, Yufei Su, and Gregory W Characklis. Assessing the bonneville power administration's financial vulnerability to hydrologic variability. *Journal of Water Resources Planning and Management*, 148(10):05022006, 2022.

[60] RI Cuppari, S Denaro, Y Su, JD Kern, and Characklis GW. Comparing alternatives for managing hydrometeorological financial risk for hydropower suppliers. *Journal of Water Resources Planning and Management*, In Review.

[61] David Hadka and Patrick Reed. Borg: An auto-adaptive many-objective evolutionary computing framework. *Evolutionary computation*, 21(2):231–259, 2013.

[62] Jazmin Zatarain Salazar, Patrick M Reed, Jonathan D Herman, Matteo Giuliani, and Andrea Castelletti. A diagnostic assessment of evolutionary algorithms for multi-objective surface water reservoir control. *Advances in water resources*, 92: 172–185, 2016.

[63] David Hadka and Patrick Reed. Large-scale parallelization of the borg multiobjective evolutionary algorithm to enhance the management of complex environmental systems. *Environmental Modelling & Software*, 69:353–369, 2015.

[64] Vira Chankong and Yacov Y Haimes. *Multiobjective decision making: theory and methodology*. Courier Dover Publications, 2008.

[65] Benjamin F Hobbs, Vira Chankong, Wael Hamadeh, and Eugene Z Stakhiv. Does choice of multicriteria method matter? an experiment in water resources planning. *Water Resources Research*, 28(7):1767–1779, 1992.

[66] Lea Kosnik. The anticommons and the environment. *Journal of environmental management*, 101:206–217, 2012.

[67] Lea Kosnik. Balancing environmental protection and energy production in the federal hydropower licensing process. *Land Economics*, 86(3):444–466, 2010.